Protein Science (1997), *6*:2336–2343. Cambridge University Press. Printed in the USA.

Kinase conformations: A computational study of the effect of ligand binding

VOLKHARD HELMS AND J. ANDREW MCCAMMON

Department of Chemistry and Biochemistry, and Department of Pharmacology, University of California at San Diego, La Jolla, California 92093-0365

(RECEIVED March 12, 1997; ACCEPTED July 24, 1997)

Abstract

Protein function is often controlled by ligand-induced conformational transitions. Yet, in spite of the increasing number of three-dimensional crystal structures of proteins in different conformations, not much is known about the driving forces of these transitions. As an initial step toward exploring the conformational and energetic landscape of protein kinases by computational methods, intramolecular energies and hydration free energies were calculated for different conformations of the catalytic domain of cAMP-dependent protein kinase (cAPK) with a continuum (Poisson) model for the electrostatics. Three protein kinase crystal structures for ternary complexes of cAPK with the peptide inhibitor PKI(5-24) and ATP or AMP-PNP were modeled into idealized intermediate and open conformations. Concordant with experimental observation, we find that the binding of PKI(5-24) is more effective in stabilizing the closed and intermediate forms of cAPK than ATP. PKI(5-24) seems to drive the final closure of the active site cleft from intermediate to closed state because ATP does not distinguish between these two states. Binding of PKI(5-24) and ATP is energetically additive.

Keywords: cAMP-dependent protein kinase; conformational transition; Poisson electrostatics calculations

"Hinge-bending" and other displacements of protein domains have been studied experimentally by gel-filtration (Russell et al., 1990), CD (Yazawa & Noda, 1976), intrinsic fluorescence spectroscopy (Tomasselli & Noda, 1983; Lew et al., 1997), time-resolved fluorescence energy transfer (Haran et al., 1992; Haas, 1996), ESR with spin labels (Mchaourab et al., 1997), neutron (Parello et al., 1993) and small-angle X-ray scattering (Pickover et al., 1979; Olah et al., 1993), time-resolved X-ray crystallography (Stoddard, 1996), and by NMR spectroscopy (Palmer et al., 1996). Insight into the structural mechanisms can be gained from the growing number of examples where multiple crystal structures of a protein in different conformations have been determined (Huber & Bennett, 1983; Lesk & Chothia, 1984; Gerstein et al., 1994). Computational studies of domain motions have also been described, although most of these have used highly approximate models for solvation effects (McCammon et al., 1976; Mao et al., 1982; Grubmueller, 1994; Schlitter et al., 1994; Perahia & Mouawad, 1995; Elamrani et al., 1996; Garcia & Harman, 1996). Yet, our knowledge about the time scales of domain motions, and about the underlying driving forces, is still very limited. In this work, we attempt to calculate conformational free energy differences for a well-suited model system, the catalytic subunit of cAMP-dependent protein kinase, which has been crystallized in three different conformations. Our main focus is on how ligand binding shifts the equilibrium among the three protein conformations.

Protein kinases catalyze the transfer of phosphate from ATP to protein substrates and are regulatory elements of most known pathways of signal transduction. The best characterized member of this large family is cAPK. It was discovered as a component in the regulation of glycogen metabolism, and more recently has been demonstrated to be directly involved in cell cycle control (Grieco et al., 1996) and in the phosphorylation and activation of transcription factors (Montminy et al., 1990). In vivo, cAPK exists as an inactive tetrameric holoenzyme that, upon binding cAMP, undergoes dissociation to a single dimeric regulatory subunit and two free, active catalytic subunits. The catalytic subunit can be inhibited potently by the peptide PKI, and by the 20-residue fragment PKI(5-24).

The catalytic subunit of cAPK was the first kinase structure determined by X-ray crystallography (Knighton et al., 1991). It consists of two domains, the "small lobe" and "large lobe," that are connected by a peptide linker. ATP binds in a deep cleft between the two domains. All but one crystallographic structure also contain a 20-residue fragment, PKI(5-24) bound on the protein surface in proximity of the binding cleft (Taylor & Radzio-Andzelm, 1994).

Reprint requests to: Volkhard Helms, Department of Chemistry and Biochemistry, University of California at San Diego, 9500 Gilman Drive, La Jolla, California, 92093-0365; e-mail: vhelms@ucsd.edu.

Abbreviations: cAPK, cAMP-dependent protein kinase; PKI, protein kinase inhibitor; ATP, adenosine deoxynucleotide triphosphate; AMP-PNP, adenylyl imidodiphosphate.

In these structures, cAPK is found in three different conformations, (1) a closed conformation in the ternary complex with ATP and PKI(5-24), in the ternary complex with ADP and PKI(5-24), and in the binary complex of recombinant cAPK with PKI(5-24), (2) an intermediate conformation in the binary complex with adenosine, and (3) an open conformation in the binary complex of mammalian cAPK with PKI(5-24). Although the angle formed by the two domains opens by ca. 15° between the crystal structures of the closed and open forms, data from low-angle X-ray scattering experiments of cAPK alone in solution indicated an opening of as much as 39° (Olah et al., 1993). The conformational transition between the open and closed crystal structures has been described on a structural level in great detail by Cox et al. (1994). Not surprisingly, the transition apparently involves not only the hinge movement of the two domains relative to each other, but also a number of more subtle structural changes in the glycine-rich loop, the C-helix, the activation loop, and so forth. Still, both domains superimpose quite well and, to a first approximation, the domain movement can be regarded as a rigid-body movement.

Transitions between different conformational states of a folded protein have been studied previously by a variety of theoretical methods. McCammon et al. (1976) studied the hinge-bending mode in lysozyme on a potential energy surface that was obtained by adiabatic mapping. Normal mode analysis was used extensively to study transitions of allosteric proteins by Go, Perahia, and co-workers (compare, e.g., Ikura & Go, 1993 and Mouawad & Perahia, 1996). Solvent effects were usually neglected in these calculations. Conventional molecular dynamics simulations in explicit solvent, on the other hand, cannot yet be extended to the microsecond to millisecond time scales typical for large domain motions. Various methods have been devised, therefore, to speed up the time scales of protein motions observed. Grubmueller (1994) described a method to induce conformational transitions in proteins and derived rate constants for these. Schlitter and co-workers (1994) described the method of targeted molecular dynamics where the direction of the transition is preset at the beginning of the simulation. Elamrani and co-workers (1996) described a simulation of adenylate kinase, a model system of a hinge-bending protein. To speed up conformational transitions, all atomic masses were scaled by a large factor, thus allowing the use of a high simulation temperature of 2,000 K. Here, elements of secondary structure had to be constrained to prevent protein unfolding. We are eventually interested in using the recently developed Poisson–Boltzmann Stochastic Dynamics method (Gilson et al., 1995) to study the dynamic domain motion of protein kinase. In this study, we perform energy calculations on static configurations using the same energy function that will be used in this latter study.

Poisson–Boltzmann electrostatics calculations are used widely nowadays to study electrostatic phenomena of biomolecules. The broad variety of applications is described in a number of recent reviews (Madura et al., 1994; Tomasi & Persico, 1994; Gilson, 1995; Honig & Nicholls, 1995). Especially, continuum electrostatics calculations have been combined with an empirical surface term that accounts for apolar solvation solvation effects to reproduce hydration free energies of small model compounds (Simonson & Brünger, 1994; Sitkoff et al., 1994). By also including intramolecular energies calculated from a molecular-mechanics force field, the range of applications has been extended to study the conformational equilibria of small peptides (Hempel et al., 1995), of protein loops (Smith & Honig, 1994), and of α-helices (Yang & Honig, 1995) and β-sheets (Yang et al., 1995). Here, we use a similar model to obtain estimates of the conformational free energy of different protein kinase conformations. The continuum description of the solvent yields a free energy including entropic solvent effects. However, intramolecular entropy differences between different protein kinase conformations are not accounted for, nor is the entropic contribution for the displacement of bound solvent molecules during conformational transitions. Although theoretical methods have been described to compute binding entropies in a rigorous fashion (Gilson et al., 1997), detailed applications to systems the size of proteins are not yet easily made. By comparing relative differences of conformational energies, it is assumed that many of the neglected contributions to the free energy will cancel out.

Grant et al. (1996) and Tsigelny et al. (1996) have performed parallel site-directed mutagenesis and electrostatic calculations on the ternary cAPK complex and have studied in detail the interactions important for substrate binding to the closed form of cAPK. In the present work, we use theoretical methods to identify driving forces for the observed domain hinge motion coupled to ligand binding, and thus complement experimental results. How does binding of PKI(5-24) and ATP shift the equilibrium toward the closed form of the enzyme? Why is the open state more favorable in the absence of ligands? Calculations were performed for the unbound protein, for binary complexes with ATP and with PKI(5-24), and for a ternary complex with ATP and with PKI(5-24). In order to check the validity of the modeling procedure, independent calculations were done starting with three different crystal structures with the closed cAPK conformation.

Results and discussion

Energy minimizations

All structures (crystal structures and modeled "intermediate" and "open" configurations) of unliganded cAPK and of complexes with ATP and PKI(5-24) were subjected individually to 500 steps of unrestrained energy minimization. As an example of a typical minimization, we show the individual energy components for the modeled "open" conformation of 1ATP in Figures 1 and 2. The coulombic energies are relatively small in magnitude due to the use of a distance-dependent dielectric constant of $5*r$. By visual inspection, all energy terms seem to converge well, except for the proper dihedral energy and the van der Waals energy terms. Energy minimizations of proteins are virtually impossible to fully converge, as noted in a recent study on BPTI (Troyer & Cohen, 1995). The purpose of the minimizations in this work was to remove local strain left after refinement of the experimental structure or caused by our crude modeling procedures.

Electrostatic calculations

Single-point energy calculations were performed for the different energy-minimized conformations of cAPK in the unbound state, in a binary complex with ATP, in a binary complex with PKI(5-24), and in a ternary complex with ATP and PKI(5-24). Electrostatic hydration free energies, the solvation contribution due to exposed apolar surface, and intramolecular energies were computed with the UHBD program (Davis et al., 1991; Madura et al., 1995). Table 1 lists the individual energy components for the various conformations.

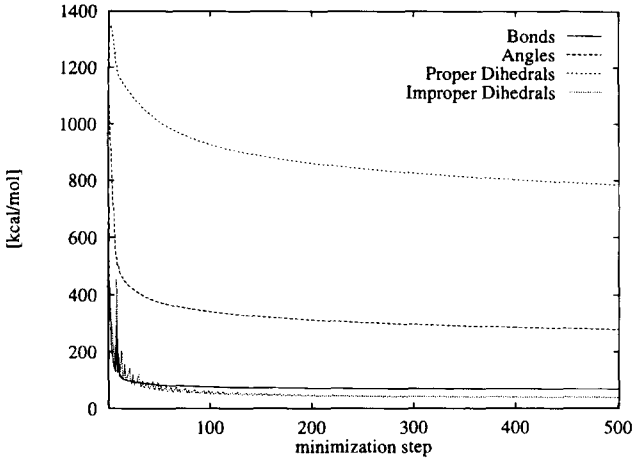

Fig. 1. Covalent intrasolute energy components during the minimization of the intermediate conformation of 1ATP with the CHARMm program.

Generally, the angle energies and proper dihedral energies are lower for the two 1CDK structures than for 1ATP. Also, vdW energies and Poisson free energies are consistently lower for the 1CDK structures than for 1ATP, whereas the coulombic energies are higher. The two proteins differ in nine amino acid positions, but the energetic differences might also reflect the use of different refinement protocols during the crystallographic structure determination. For unbound cAPK, the total conformational free energies increase monotonically for all three systems studied in the sequence closed–"intermediate"–"open" and "open" with 1cmk-loop. With the exception of the Poisson free energy of hydration that favors the solvation of buried protein groups, this trend is also true for the individual energy components.

The "open" conformation with the C-terminal tail from 1CMK.pdb has significantly higher conformational free energies (ca. 250–300 kcal/mol) than the "open" conformation with the C-terminal tail from 1ATP.pdb. The moderate gain in Poisson solvation free energy in this case does not compensate for the significant loss mostly in intramolecular coulombic energy. As mentioned before, we do not account for entropic contributions in our model such as conformational flexibility that may be larger for the 1CMK-C-terminal tail. In the following, we only show the data for protein complexes in the open conformation with the 1ATP-loop because both systems are always separated by a similar energy as for unbound cAPK.

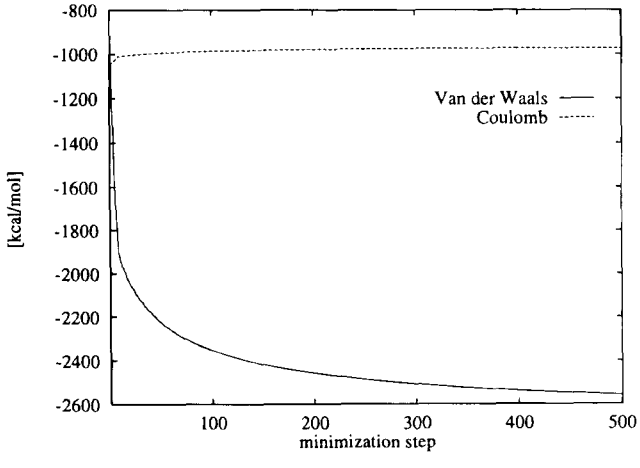

Fig. 2. As in Figure 1, noncovalent intrasolute energy components.

In the ligand complexes, intramolecular covalent energies are slightly higher than in the unbound protein. This is simply due to the larger number of atoms, and the effects of including ATP and PKI(5-24) are, to a good approximation, additive. As expected, the noncovalent energies are more favorable in the complexes. The binary complexes with ATP or PKI(5-24) have lower coulombic energies than unbound cAPK by ca. 1,000 (PKI) and 1,100 (ATP) kcal/mol. The difference in van der Waals energy is ca. 180 kcal/mol for the complex with PKI(5-24) and ca. 30 kcal/mol in the complex with ATP. The Poisson free energies are more favorable for the binary complexes by 95–130 kcal/mol, although ATP is almost fully shielded from solvent. For ATP, this might be partly due to the small cavities close to the ligand, usually filled with crystal waters, that are now treated as solvent dielectric.

Choosing three different crystal structures, the same trends were observed. This provides confidence in the combination of modeling and energy calculations for studying different conformational states of a protein.

The ranking of total conformational free energies indicates that the closed state of cAPK is favored even in the absence of ligands, which is in contrast to experimental data, e.g., from small-angle X-ray diffraction (Parello et al., 1993), that show a preferred population of the open conformation. One reason for this discrepancy could be that the modeled "intermediate" and "open" states do not correspond to real states. That is, the energies of real intermediate and open states might be lower. We have included the free energies calculated for the 1BKX.pdb crystal structure in Table 1. They are far more unfavorable than those of the modeled intermediate state. This shows that using real crystal structures can be problematic for studying idealized problems, such as the energetics in a hinge motion. For example, proteins do not necessarily have to adopt a unique conformation in their open state (Gerstein et al., 1994). Another more likely reason might be the omission of important contributions to the conformational free energy in our calculations, such as the contribution of the water molecules that are released from the binding cleft upon closure, or the entropy of the protein in different conformations. In the discussion below, by comparing relative energy differences for different ligation states of the protein rather than absolute energies, we assume that most these omitted terms cancel.

We thus concentrated on how the energy ranking of states is affected by the binding of the peptide inhibitor and ATP. The averages of the conformational free energies of the intermediate and open states of cAPK were calculated relative to that of the closed state, and the results are shown in Figure 3. The intermediate conformations of cAPK:ATP and cAPK are separated by a similar energy gap from the closed conformations, indicating that ATP binding does not substantially shift the equilibrium between the intermediate and the closed state. This appears reasonable in light of the crystallographic structures because the contacts between cAPK and ATP are hardly affected by this moderate opening of the binding cleft. The open state is disfavored by ca. 25 kcal/mol when ATP is bound. Binding of PKI(5-24), on the other hand, clearly stabilizes the closed state over the intermediate state by ca. 15 kcal/mol and over the open state by ca. 60 kcal/mol. The energy gaps between the open states of cAPK:ATP and cAPK (26

Table 1. *Individual energy components for different cAPK conformations (kcal/mol)*[a]

System	Bond	Angle	Prop. dih.	Imp. dih.	ΔG_{cov}	vdW	Coul.	PB	Surf.	ΔG_{noncov}	ΔG_{total}
A. Unliganded cAPK											
1ATP	67.6	277.2	791.2	37.9	1,173.9	−2,590.5	−13,520.3	−3,014.0	87.7	−19,037.1	−17,863.2
1ATP-I	67.4	278.2	784.7	38.3	1,168.6	−2,579.8	−13,476.4	−3,039.2	87.7	−19,007.7	−17,839.1
1BKX	69.8	298.4	865.7	39.9	1,273.8	−2,474.8	−13,104.3	−3,199.1	91.2	−18,687.0	−17,413.2
1ATP-O	67.7	283.0	792.2	38.9	1,181.8	−2,559.0	−13,474.6	−3,030.8	89.5	−18,974.9	−17,793.1
1ATP-OL	68.6	293.1	803.0	40.6	1,205.3	−2,510.5	−13,011.8	−3,252.4	92.6	−18,682.1	−17,476.8
1CDKA	66.8	263.2	734.9	35.0	1,099.9	−2,605.7	−13,180.7	−3,193.6	90.4	−18,889.6	−17,789.7
1CDKA-I	66.8	264.1	743.5	35.5	1,109.9	−2,588.5	−13,180.7	−3,193.7	90.4	−18,872.5	−17,762.7
1CDKA-O	66.7	265.6	741.0	35.9	1,109.2	−2,570.8	−13,189.7	−3,190.0	92.8	−18,857.7	−17,748.5
1CDKA-OL	67.5	275.0	750.2	39.4	1,132.1	−2,532.4	−12,842.3	−3,345.3	94.4	−18,625.6	−17,493.5
1CDKB	66.7	261.5	711.4	33.9	1,073.5	−2,603.8	−13,285.3	−3,151.5	91.3	−18,949.3	−17,875.8
1CDKB-I	66.9	261.7	710.6	34.5	1,073.7	−2,590.6	−13,231.8	−3,177.3	91.3	−18,908.4	−17,834.7
1CDKB-O	67.0	263.0	711.4	34.6	1,076.0	−2,575.4	−13,238.5	−3,169.7	93.8	−18,889.8	−17,813.8
1CDKB-OL	67.1	274.1	724.6	37.7	1,103.5	−2,536.3	−12,875.4	−3,338.5	95.5	−18,654.7	−17,551.2
B. Binary cAPK:ATP complexes											
1ATP	69.5	303.1	824.9	43.2	1,240.7	−2,618.0	−14,614.2	−3,114.2	86.4	−20,260.0	−19,019.3
1ATP-I	69.7	303.5	821.4	44.3	1,238.9	−2,601.9	−14,592.4	−3,134.7	86.5	−20,242.5	−19,003.6
1ATP-O	69.7	310.1	827.5	45.0	1,252.3	−2,567.5	−14,537.3	−3,155.4	87.4	−20,172.8	−18,920.5
1CDKA	68.9	289.3	761.4	40.9	1,160.5	−2,642.9	−14,259.8	−3,300.4	89.2	−20,113.9	−18,953.4
1CDKA-I	69.0	290.1	767.8	41.5	1,168.4	−2,621.3	−14,245.7	−3,306.3	89.2	−20,084.1	−18,915.7
1CDKA-O	68.7	291.6	770.9	41.5	1,172.7	−2,589.6	−14,244.4	−3,315.6	91.2	−20,058.4	−18,885.7
1CDKB	68.7	286.7	736.4	40.0	1,131.8	−2,643.2	−14,369.2	−3,255.9	90.0	−20,178.3	−19,046.5
1CDKB-I	68.5	286.2	735.9	40.1	1,130.7	−2,625.3	−14,331.6	−3,278.9	90.0	−20,145.8	−19,015.1
1CDKB-O	68.7	288.4	737.9	39.9	1,134.9	−2,595.4	−14,303.1	−3,292.5	92.0	−20,099.0	−18,964.1
C. Binary cAPK:PKI(5-24) complexes											
1ATP	70.6	289.2	831.3	39.7	1,230.8	−2,771.0	−14,539.1	−3,101.1	88.8	−20,322.4	−19,091.6
1ATP-I	70.6	289.7	823.7	39.9	1,223.9	−2,752.2	−14,454.4	−3,152.0	89.4	−20,269.2	−19,045.3
1ATP-O	70.5	294.7	831.6	40.6	1,237.4	−2,720.7	−14,377.3	−3,177.3	92.9	−20,182.4	−18,945.0
1CDKA	69.7	274.2	770.3	36.6	1,150.8	−2,784.7	−14,185.7	−3,290.0	92.0	−20,168.4	−19,017.6
1CDKA-I	69.8	274.9	777.9	37.0	1,159.6	−2,760.3	−14,162.0	−3,305.7	92.4	−20,135.6	−18,976.0
1CDKA-O	69.6	276.3	775.0	37.4	1,158.3	−2,733.3	−14,111.6	−3,328.6	96.3	−20,077.2	−18,918.9
1CDKB	69.7	272.4	744.9	35.5	1,122.5	−2,784.8	−14,275.0	−3,255.4	92.6	−20,222.6	−19,100.1
1CDKB-I	69.7	272.6	743.5	35.9	1,121.7	−2,763.5	−14,210.4	−3,289.3	93.3	−20,169.9	−19,048.2
1CDKB-O	69.7	274.0	744.4	36.1	1,124.2	−2,739.9	−14,156.2	−3,310.5	97.2	−20,109.4	−18,985.2
D. Ternary cAPK:ATP:PKI(5-24) complexes											
1ATP	72.8	315.1	864.6	45.4	1,297.9	−2,801.0	−15,619.5	−3,208.0	87.7	−21,540.8	−20,242.9
1ATP-I	73.0	315.5	859.7	46.2	1,294.4	−2,777.5	−15,557.9	−3,249.5	88.4	−21,496.5	−20,202.1
1ATP-O	73.0	322.0	866.2	46.9	1,308.1	−2,733.1	−15,445.0	−3,296.7	90.7	−21,384.1	−20,076.0
1CDKA	72.2	300.5	796.8	42.5	1,212.0	−2,825.2	−15,254.0	−3,403.8	90.9	−21,392.1	−20,180.1
1CDKA-I	72.3	301.2	802.6	42.9	1,219.0	−2,795.8	−15,211.3	−3,427.5	91.4	−21,343.2	−20,124.2
1CDKA-O	72.0	302.7	805.5	43.1	1,223.3	−2,755.6	−15,161.1	−3,454.2	94.3	−21,276.6	−20,053.3
1CDKB	71.9	298.2	769.3	41.7	1,181.1	−2,827.7	−15,369.4	−3,355.6	91.5	−21,461.2	−20,280.1
1CDKB-I	71.8	297.8	767.9	41.8	1,179.3	−2,801.2	−15,313.4	−3,391.4	92.2	−21,413.8	−20,234.5
1CDKB-O	71.9	299.6	770.7	41.5	1,183.7	−2,763.5	−15,229.6	−3,427.0	95.1	−21,325.0	−20,141.3

[a] ΔG_{cov} is the sum of the covalent bond, bond angle, proper dihedral, and improper dihedral energies. ΔG_{noncov} is the sum of the noncovalent intramolecular van der Waals and coulombic energies, the Poisson (PB) hydration free energy, and the apolar hydration free energy due to solvent-exposed surface. ΔG_{total} is the sum of ΔG_{cov} and ΔG_{noncov}. Names of the simulation systems are explained in Table 2.

kcal/mol) and between cAPK:PKI(5-24):ATP and cAPK:PKI(5-24) (24 kcal/mol) are very similar, indicating that ATP and PKI(5-24) do not interact significantly in the bound state.

The averaging of the energies calculated for the three proteins might be questionable because the standard deviations of the calculated average energies are of similar size as the differences between the energies of closed and intermediate states (not shown). Yet for the open state, the same ranking of free energies is obtained for each of the three structures separately. Thus, the same conclusion can be drawn from the results for a single structure as for the average of the three structures. The trends are also visible for the intermediate states, although here the order of cAPK and cAPK:ATP, and of cAPK:PKI(5-24) and cAPK:PKI(5-24):ATP is different for the three structures.

By applying the same averaging procedure to individual free energy contributions, one could, in principle, identify the key driving forces for binding. Unfortunately, the large spread among the three systems does not allow definitive statements. Certainly no

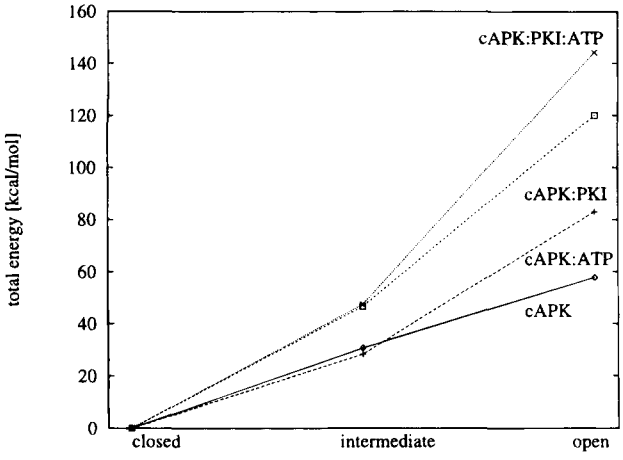

Fig. 3. Conformational free energy of closed, intermediate, and open protein kinase conformation. "cAPK" indicates the unbound form of cAMP-dependent protein kinase; "cAPK:ATP," the binary complex of cAPK with ATP; "cAPK:PKI," the binary complex of cAPK with the peptide inhibitor PKI(5-24); and "cAPK:PKI:ATP," the ternary complex of cAPK with ATP and PKI(5-24). Shown are averaged values for the three crystal structures 1ATP.pdb, 1CDKA.pdb, and 1CDKB.pdb. All values have been normalized with respect to the free energy of the closed conformations.

single effect clearly dominates, and the conformational transition is due to a complex interplay of various contributions.

Biological relevance

The calculated conformational free energies indicate that both ATP and PKI(5-24) disfavor the open state with regard to intermediate and closed state. Binding of PKI(5-24) seems to drive the complete closing of the binding cleft from the intermediate to the closed state. This is in accord with data from small-angle neutron scattering that showed that the binding of inhibitor peptide, but not ATP alone, was sufficient to cause the reduction in the protein radius of gyration (Parello et al., 1993).

We here point out that the calculated conformational free energies cannot be compared easily with experimental K_d values because ATP and PKI(5-24) can, in principle, bind to different conformations of cAPK, and these conformational analyses do not reflect certain entropy contributions to K_d, as described above. Experimentally, ATP bound 2,000 times stronger to cAPK in the presence of PKI(5-24) than in the absence of PKI(5-24) (7.3 nM versus 25 μM) (Lew et al., 1997), which corresponds to a 4.8 kcal/mol difference in binding free energy. This strong synergism was ascribed previously to an extended network between the PKI N-terminus and the ATP binding site (Lew et al., 1997).

In our study, intradomain protein motion was practically excluded except for small refinements during energy minimization, and the calculated conformational free energies are solely due to domain opening and closure. The binding of ATP and PKI(5-24) was calculated to be energetically independent. Yet, the magnitude of the experimentally observed synergism is smaller than typical energy differences between different protein conformations and ligation states, and the synergism may not be detectable in such a study.

In a subsequent publication, we will address the role of the flexibility of the Gly-rich loop. It is known (Narendra et al., 1997a) that this small loop is involved in substrate recognition. Preliminary calculations show that its influence on the calculated energies is much smaller than that of the various cAPK calculations. We will also address the role of the phosphorylated residues Thr 197 and Ser 338 and the effect of treating some of the crystallographic solvent molecules close to ATP in an explicit way. These values will eventually be compared with results from ongoing fluorescence resonance energy transfer experiments (J. Lew, B. Grant, & S.S. Taylor, in prep.).

Materials and methods

Free energy function

The conformational free energy was estimated by the following energy expression, analogous to previous work (Gilson et al., 1995; Marrone et al., 1996): $\Delta G_{confE} = \Delta G_{bond} + \Delta G_{angle} + \Delta G_{prop.\ dih} + \Delta G_{improp.\ dih} + \Delta G_{vdW} + \Delta G_{coul} + \Delta G_{PB} + \Delta G_{surf}$. Here, ΔG_{bond}, ΔG_{angle}, $\Delta G_{prop.\ dih}$, and $\Delta G_{improp.\ dih}$ are equal to the covalent intramolecular energies for bond stretching, angle bending, and for the out-of-plane bending of proper and improper dihedral angles. ΔG_{vdW} and ΔG_{coul} are the noncovalent intrasolute van der Waals and coulombic energies. These energy terms were all evaluated by the molecular mechanics force field CHARMm22 after energy minimizing the molecule as described below. ΔG_{PB} is the electrostatic free energy of hydration evaluated by the UHBD program as described below. The apolar solvation free energy ΔG_{surf} was calculated within the UHBD program from the solvent-accessible surface area of the molecule multiplied by the factor 25 J/(mol-Å^2).

Crystal structures used in this study

"Open" and "intermediate" refer to modeled chimeric structures, as defined below, whereas open and intermediate refer to the crystallographically observed structures.

Three crystal structures of ternary complexes of cAPK with the 20-residue fragment of a peptide inhibitor, PKI(5-24), and with either ATP or MnAMP-PNP were used as models for the closed state of cAPK. The ternary complex of the recombinant mouse form (Zheng et al., 1993a), 1ATP, was determined at 2.2 Å resolution. 1CDK (Bossemeyer et al., 1993) is a 2.0-Å resolution structure of a ternary complex of a pig form of cAPK with the ATP-analogue AMP-PNP and PKI(5-24) bound (Bossemeyer et al., 1993). 1ATP and 1CDK were determined in different laboratories. The sequences of the pig and the mouse forms of cAPK differ in nine positions, but all mutations are conservative. The only difference between AMP-PNP and ATP is the replacement of the oxygen atom that links P_β and P_γ by a nitrogen atom. Both ATP and AMP-PNP are coordinated by two Mn^{2+} ions that neutralize their net charge of −4. 1CDK contains two cAPK complexes per unit cell that were refined independently, which will be termed 1CDKA and 1CDKB. The RMS deviation between 1CDKA and 1CDKB is 0.28 Å (nonhydrogen atoms), between 1CDKA and 1ATP, 0.43 Å, and between 1CDKB and 1ATP, 0.41 Å.

The crystal structure of the binary complex of cAPK with adenosine (Narendra et al., 1997b) was chosen as a template for an "intermediate" conformation of protein kinase. This structure, 1BKX, was determined recently at 2.6 Å resolution. As templates for "open" conformations of cAPK, we have used the two structures of binary complexes of mammalian cAPK with PKI(5-24), 1CTP, and 1CMK that were determined at 2.9 Å resolution (Zheng et al., 1993b). Many surface residue side chains were not visible

in the electron density of these relatively low-resolution structures. However, because many of them are charged, they cannot simply be neglected in electrostatic calculations. Modeling of their orientation would introduce some arbitrariness into the calculations, on the other hand. Instead of performing calculations for the different crystal structures, we decided to use a strategy that involved mapping the domains of the highly resolved structures onto the intermediate and open frameworks. Thus, the calculated energy differences are due solely to the opening and closing mechanism.

Modeling of protein kinase

The crystal structures 1ATP, 1CDKA, and 1CDKB of the ternary complexes of cAPK are among those with the highest crystallographic resolution. They were modeled into "intermediate" and "open" conformations by superimposing the two domains on those of the intermediate 1BKX or open 1CTP structures with the INSIGHT program (v. 2.7; Biosym/MSI, San Diego, California), and then constructing appropriate peptide linkages. Because the glycine-rich loop (residues 50–57) seems to move independently from the small lobe (Narendra et al., 1997b), only residues 60–120 in the small domain were used for the superposition of the small lobe.

The two domains of cAPK are connected by a peptide linker, Met 120–Glu 127, and by the Pro 316–Glu 331 piece of the C-terminal tail. The conformations of the linker in the closed, intermediate, and open conformations, are quite similar, as shown in Figure 4. Second, the conformation of the C-terminal tail is not included in 1CTP and was only visible as weak electron density in the open 1CMK configuration. Here, it is not simply rotated and translated with respect to the closed 1ATP conformation, but it adopts a different backbone configuration. Yet, its endpoints are close to those of the C-terminal tail in the closed 1ATP structure, and, fortunately, none of the point mutations between pig and mouse cAPK are located in the C-terminal tail. Therefore, two strategies were adopted for the modeling of the C-terminal tail region between the large lobe and the rotated small lobe. First, we used the conformation of the C-terminal tail in the closed structure. Second, the conformation of the C-terminal tail [residues 312–339 (1ATP), 312–341 (1CDKA), or 309–339 (1CDKB)] in the open 1CMK conformation was used. Figure 5 shows a superposition of the two alternative conformations of the C-terminal tail in the modeled "open" conformation of 1ATP.

Fig. 4. Closed conformation of c-AMP dependent protein kinase (yellow), intermediate conformation (green), and open conformation (white) were superimposed on the large lobe. Conformations of the linker are shown as RIBBON drawings.

Fig. 5. Two modeled "open" conformations of 1ATP. For the white structure, the C-terminal tail was taken from 1ATP.pdb, whereas for the yellow structure, that of 1CMK.pdb was adopted.

The N-terminal helix is attached to the small lobe. Its position is therefore displaced from its crystal position in the modeled "intermediate" and "open" conformations. The deviations are between ca. 1.7 Å for the "intermediate" conformation and ca. 8 Å for the "open" conformation, where the latter structures are those derived from 1CDKB. The conformation of residues 15–23 or residues 15–30 was taken from the closed conformation, depending on which procedure resulted in a better fit. The N-terminal helix is located on the opposite side of the active site, and its exact position is not expected to affect the results of this study signifi-

cantly, because only relative energy differences are compared. In all crystal structures, the N-terminal α-helix is only partly visible. In order to facilitate the comparison, the first 14 residues were removed in all protein structures during this study, although, in some of the structures, only the first 7 residues are missing.

The protonation state of the histidine residues was assigned by graphical analysis of their environment in the closed complexes. N- and C-terminal capping groups were added to cAPK and PKI(5-24) by the QUANTA program (v. 4.0; Molecular Simulations, Inc., San Diego, California). Crystal waters were not included in the calculations. Thr 197 and Ser 338 were treated as unphosphorylated.

Table 2 gives a summary of all modeled structures, and lists the short names used in this study.

Refinement of modeled structures by energy minimization

Polar hydrogens were added with the HBUILD algorithm within the CHARMm program (v. 22.2; Harvard College) and their positions were optimized by 500 steps of steepest-descent energy minimization. In a second optimization, all atomic coordinates were subjected to 500 steps of steepest-descent energy minimization. During this minimization, a dielectric constant of $5*r$ was employed to model solvent effects and to reduce the driving force of the coulombic forces. The commercial variant of the CHARMm22 force field (Quanta 4.0 handbook; Molecular Simulations, Inc., Waltham, Massachusetts) was used for these calculations because it has been used in a number of continuum calculations, it contains parameters for all fragments (ATP, Mn^{2+} ions), and it is conveniently interfaced with the UHBD program. For simplicity, the same parameters were used for AMP-PNP as for ATP. In the following, "ATP" will be used both for $2Mn^{2+}$ATP and $2Mn^{2+}$AMP-PNP.

Electrostatic calculations

The UHBD program was used to calculate hydration free energies by solving the Poisson equation with the finite difference technique. Atomic radii and partial atomic charges were taken from the CHARMm22 force field. After orienting the protein favorably within the cubic box, the dimensions of 1ATP were 60.0 × 59.9 × 61.3 Å^3. In order to be able to use a reliably small grid spacing, it was necessary to use larger grid dimensions than are being used routinely. Table 3 lists the memory requirements and CPU time for Poisson calculations of 200 iterations with different grid sizes. Also, the calculated ΔG_{hydr} are shown for the different grid sizes. Apparently, they are well converged for a grid spacing of 0.3 Å. All further calculations in this work employed a cubic 240 × 240 × 240 grid. The protein dielectric constant in the continuum calculations was 2 and the solvent dielectric constant was 78. Intramolecular energies were evaluated within UHBD with the commercial version of the CHARMm22 force field. Here, the dielectric constant of protein and solvent was 1.

Table 2. *Names and descriptions of all structures used for energy calculations*[a]

System	Domain conformation	C-terminal tail	Name used
1ATP	Closed	1ATP	1ATP
1ATP	Intermediate	1ATP	1ATP-I
1ATP	Open	1ATP	1ATP-O
1ATP	Open	1CMK	1ATP-OL
1CDKA	Closed	1ATP	1CDKA
1CDKA	Intermediate	1ATP	1CDKA-I
1CDKA	Open	1ATP	1CDKA-O
1CDKA	Open	1CMK	1CDKA-OL
1CDKB	Closed	1ATP	1CDKB
1CDKB	Intermediate	1ATP	1CDKB-I
1CDKB	Open	1ATP	1CDKB-O
1CDKB	Open	1CMK	1CDKB-OL
1BKX	Intermediate	1BKX	1BKX

[a]Structures with "I" attached are intermediate structures and structures with "O" attached are open structures. "L" indicates that the C-terminal tail was taken from 1CMK.pdb.

Table 3. *Memory and CPU requirements for a single Poisson calculation*

Grid spacing (Å)	Grid dimension	Size of UHBD executable (Mbyte)	CPU time on SGI RS10000 (s)	Poisson ΔG_{hydr} (kcal/mol)
0.5	150	359	1,961	−3,030.2
0.4	180	487	3,689	−3,015.8
0.35	210	665	5,819	−3,017.5
0.3	240	903	10,098	−3,014.0

Acknowledgments

Dr. Narayana Narendra kindly provided the coordinates of the binary complex of cAPK with adenosine prior to publication. We thank Dr. Tami Marrone, Dr. Narayana Narendra, Dr. Angel Ortiz, and members of the research group of Dr. Susan Taylor for valuable discussions, and Dr. John Lew and Dr. Elzbieta Radzio-Andzelm for critical reading of the manuscript. This work was supported by a postdoctoral NATO fellowship to V.H. by the Deutscher Akademischer Austauschdienst, and by grants from NIH, NSF, and the NSF Supercomputer Centers MetaCenter program.

References

Bossemeyer D, Engh RA, Kinzel V, Ponstingl H, Huber R. 1993. Phosphotransferase and substrate binding mechanism of the CAMP-dependent protein kinase catalytic subunit from porcine heart as deduced from the 2.0 Å structure of the complex with mn^{2+} adenylyl imidodiphosphate and inhibitor peptide pki(5-24). *EMBO J 12*:849–859.

Cox S, Radzio-Andzelm E, Taylor SS. 1994. Domain movements in protein kinases. *Curr Opin Struct Biol 4*:893–901.

Davis ME, Madura JD, Luty BA, McCammon JA. 1991. Electrostatics and diffusion of molecules in solution: Simulations with the University of Houston Brownian dynamics program. *Comput Phys Commun 62*:187–197.

Elamrani S, Berry MB Jr, GN Phillips, McCammon JA. 1996. Study of global motions in proteins by weighted masses molecular dynamics: Adenylate kinase as a test case. *Proteins Struct Funct Genet 25*:79–88.

Garcia AE, Harman JG. 1996. Simulations of CRP:$(CAMP)_2$ in noncrystalline environments show a subunit transition from the open to the closed conformation. *Protein Sci 5*:62–71.

Gerstein M, Lesk AM, Chothia C. 1994. Structural mechanisms for domain movements in proteins. *Biochemistry 33*:6739–6749.

Gilson MK. 1995. Theory of electrostatic interactions in macromolecules. *Curr Opin Struct Biol 5*:216–223.

Gilson MK, Given JA, Bush BL, McCammon JA. 1997. The statistical-thermodynamic basis for computation of binding affinities: A critical review. *Biophys J 72*:1047–1069.

Gilson MK, McCammon JA, Madura JD. 1995. Molecular dynamics simulation with a continuum electrostatic model of the solvent. *J Comput Chem 16*:1081–1095.

Grant BD, Tsigelny I, Adams JA, Taylor SS. 1996. Examination of an active-site electrostatic node in the cAMP-dependent protein kinase catalytic subunit. *Protein Sci 5*:1316–1324.

Grieco D, Porcellini A, Avvedimento EV, Gottesman ME. 1996. Requirement for cAMP-PKA pathway activation by m phase-promoting factor in the transition from mitosis to interphase. *Science 271*:1718–1723.

Grubmueller H. 1994. Predicting slow structural transitions in macromolecular systems: Conformational flooding. *Phys Rev E 52*:2893–2906.

Haas E. 1996. Energy transfer methods for determining distance distributions and conformational fluctuations in proteins. In: Havel HA, ed. *Spectroscopic methods for determining protein structure in solution*. New York: VCH Publishers Inc. pp 28–61.

Haran G, Haas E, Szpikowska BK, Mas MT. 1992. Domain motions in phosphoglycerate kinase: Determination of interdomain distance distributions by site-specific labeling and time-resolved fluorescence energy transfer. *Proc Natl Acad Sci USA 89*:11764–11768.

Hempel JC, Fine RM, Hassan M, Ghoul W, Guaragna A, Koerber SC, Li Z, Hagler AT. 1995. Conformational analysis of endothelin-1: Effects of solvation free energy. *Biopolymers 36*:283–301.

Honig B, Nicholls A. 1995. Classical electrostatics in biology and chemistry. *Science 268*:1144–1149.

Huber R, Bennett WS. 1983. Functional significance of flexibility in proteins. *Biopolymers 22*:261–279.

Ikura T, Go N. 1993. Normal mode analysis of mouse epidermal growth factor: Characterization of the harmonic motion. *Proteins Struct Funct Genet 16*:423–436.

Knighton DR, Zheng J, Ten-Eyck LF, Xuong N, Taylor SS, Sowadski JM. 1991. Crystal structure of the catalytic subunit of c-AMP dependent protein kinase. *Science 253*:414–420.

Lesk AM, Chothia C. 1984. Mechanisms of domain closure in proteins. *J Mol Biol 174*:175–191.

Lew J, Coruh N, Tsigelny I, Garrod S, Taylor SS. 1997. Synergistic binding of nucleotides and inhibitors to cAMP-dependent protein kinase examined by acrylodan fluorescence spectroscopy. *J Biol Chem 272*:1507–1513.

Madura JD, Briggs JM, Wade RC, Davis ME. 1995. Electrostatics and diffusion of molecules in solution: Simulations with the University of Houston Brownian dynamics program. *Comput Phys Commun 91*:57–95.

Madura JD, Davis ME, Gilson MK, Wade RC, Luty B, McCammon JA. 1994. Biological applications in electrostatic calculations and brownian dynamics simulations. In: Lipkowitz KB, Boyd DB, eds. *Reviews in computational chemistry, vol V*. New York: VCH Publishers Inc. pp 229–267.

Mao B, Pear MR, McCammon JA, Quiocho FA. 1982. Hinge-bending in L-arabinose-binding protein. *J Biol Chem 257*:1131–1133.

Marrone T, Gilson MK, McCammon JA. 1996. Comparison of continuum and explicit models of solvation: Potentials of mean force for alanine dipeptide. *J Phys Chem 100*:1439–1441.

McCammon JA, Gelin BR, Karplus M, Wolynes PG. 1976. The hinge-bending mode in lysozyme. *Nature 262*:325–326.

Mchaourab HS, Oh KJ, Fang CJ, Hubbell WL. 1997. Conformation of T4 lysozyme in solution. Hinge-bending motion and the substrate-induced conformational transition studied by site-directed spin labeling. *Biochemistry 36*:307–316.

Montminy MR, Gonzalez GA, Yamamoto KK. 1990. Regulation of cAMP-inducible genes by creb. *Trends Neurosci 13*:184–188.

Mouawad L, Perahia D. 1996. Motions in hemoglobin studied by normal mode analysis and energy minimization: Evidence for the existence of tertiary t-like, quaternary r-like intermediate structures. *J Mol Biol 258*:393–410.

Narayana N, Cox S, Shaltiel S, Taylor SS, Xuong N. 1997a. Crystal structure of a polyhistidine-tagged recombinant catalytic subunit of cAMP-dependent protein kinase complexed with the peptide inhibitor PKI (5-24) and adenosine. *Biochemistry 36*:4438–4448.

Narayana N, Cox S, Xuong N, Ten-Eyck LF, Taylor SS. 1997b. A binary complex of the catalytic subunit of cAMP-dependent protein kinase and adenosine further defines conformational flexibility. *Structure 5*:921–935.

Olah GA, Mitchell RD, Sosnick TR, Walsh DA, Trewhella J. 1993. Solution structure of the cAMP-dependent protein kinase catalytic subunit and its contraction upon binding the protein kinase inhibitor peptide. *Biochemistry 32*:3649–3657.

Palmer AG, Williams J, McDermott A. 1996. Nuclear magnetic resonance studies of biopolymer dynamics. *J Phys Chem 100*:13293–13310.

Parello J, Timmins PA, Sowadski JM, Taylor SS. 1993. Conformational changes in the catalytic subunit of cAMP-dependent protein kinase. A small-angle neutron scattering study in solution. *J Mol Biol 253*:414–420.

Perahia D, Mouawad L. 1995. Computation of low-frequency normal modes in macro-molecules: Improvements to the method of diagonalization in a mixed basis and application to hemoglobin. *Comp Chem 19*:241–246.

Pickover CA, McKay DB, Engelman DM, Steitz TA. 1979. Substrate binding closes the cleft between the domains of yeast phosphoglycerate kinase. *J Biol Chem 254*:11323–11329.

Russell PJ Jr, Chinn E, Williams A, David-Dimarino C, Tauolane JP, Lopez R. 1990. Evidence for conformers of rabbit muscle adenylate kinase. *J Biol Chem 265*:11804–11809.

Schlitter J, Engels M, Kruger P. 1994. Targeted molecular dynamics: A new approach for searching pathways of conformational transitions. *J Mol Graph 12*:84–89.

Simonson T, Brünger AT. 1994. Solvation free energies estimated from macroscopic continuum theory: An accuracy assessment. *J Phys Chem 98*:4683–4694.

Sitkoff D, Sharp KA, Honig B. 1994. Accurate calculation of hydration free energies using macroscopic solvent models. *J Phys Chem 98*:1978–1988.

Smith KC, Honig B. 1994. Evaluation of the conformational free energies of loops in protein. *Proteins Struct Funct Genet 18*:119–132.

Stoddard BL. 1996. Intermediate trapping and Laue X-ray diffraction: Potential for enzyme mechanism, dynamics, and inhibitor screening. *Pharmacol Ther 70*:216–256.

Taylor SS, Radzio-Andzelm E. 1994. Three protein kinase structures define a common motif. *Structure 2*:345–355.

Tomasi J, Persico M. 1994. Molecular interactions in solution: An overview of methods based on continuous distributions of the solvent. *Chem Rev 94*:2027–2094.

Tomasselli AG, Noda LH. 1983. Baker's yeast adenylate kinase. *Eur J Biochem 132*:109–115.

Troyer JJ, Cohen FE. 1995. Protein conformational landscapes: Energy minimization and clustering of a long molecular dynamics trajectory. *Proteins Struct Funct Genet 23*:97–110.

Tsigelny I, Grant BD, Taylor SS, Ten-Eyck LF. 1996. Catalytic subunit of cAMP-dependent protein kinase: Electrostatic features and peptide recognition. *Biopolymers 39*:353–365.

Yang AS, Hitz B, Honig B. 1995. Free energy determinants of secondary structure formation: III: β-turns and their role in protein folding. *J Mol Biol 259*:873–882.

Yang AS, Honig B. 1995. Free energy determinants of secondary structure formation: I. α-helices. *J Mol Biol 252*:351–365.

Yazawa M, Noda LH. 1976. Studies on tyrosine residues in porcine muscle adenylate kinase. *J Biol Chem 251*:3021–3026.

Zheng J, Knighton DR, Ten-Eyck LF, Karlsson R, Xuong NH, Taylor SS, Sowadski JM. 1993a. Crystal structure of the catalytic subunit of cAMP-dependent protein kinase complexed with MgATP and peptide inhibitor. *Biochemistry 32*:2154–2161.

Zheng J, Knighton DR, Xuong NH, Taylor SS, Sowadski JM, Ten-Eyck LF. 1993b. Crystal structures of the myristylated catalytic subunit of cAMP-dependent protein kinase reveal open and closed conformations. *Protein Sci 2*:1559–1573.